CANM
ACMN

OANM

Eastern Great Lakes
Chapter-SNM

BOOK OF ABSTRACTS

Canadian Association of Nuclear Medicine

l'Association canadienne de médecine nucléaire

&

Ontario Association of Nuclear Medicine

&

Eastern Great Lakes Chapter - Society of Nuclear Medicine

April 28 - 30, 2011 / du 28 au 30 avril 2011

Niagara Falls, Ontario

001

MANAGEMENT OF CHRONIC DEPRESSION WITH BRAIN SPECT IMAGING: A CASE REPORT

Marc A. Freeman[1] and Howard Schneider[21.] Mount Sinai Hospital, Department of Nuclear Medicine, University of Toronto, Toronto, Ontario, M5G 1X5. [2.] Sheppard Associates, 649 Sheppard Avenue W, Toronto, Ontario, Canada M3H 2S4 Tel: 416-630-0610

Objectives: Can the brain SPECT images of patients with Major Depressive Disorder aid in their management?
Methods Used: Patients received approximately 400 MBq of intravenous Tc99m-HMPAO (technetium Tc99m exametazime/hexamethylpropylene amine oxime). A 20 minute continuous scan was performed with a Picker Prism 3000XP triple head gamma camera using an ultra-high resolution collimator. Odyssey 3D rendering software was then used to create the final images.
What we term "3D SPECT" combines the scanning data via thresholding functions to synthesize a 3D model of the brain as follows: pixels representing the top 45% of tracer activity are used in the outside cortical 3D surface view of the brain, and the top 8%, 15% and 45% pixels create the 3D view of the functional interior of the patient's brain.
Results Obtained: 70 community-based psychiatric patients with varying degrees of resistant depressive symptoms underwent 3D brain SPECT scans. The following patterns were observed:
i. Thalamic hyperactivity
ii. Thalamic hyperactivity plus prefrontal cortical hypoactivity
iii. Global overactivity suggestive of a bipolar spectrum disorder
iv. Thalamic hyperactivity plus scattered regions of cortical hypoactivity
v. Thalamic hyperactivity plus basal ganglia hyperactivity
vi. Thalamic hyperactivity plus anteromedial temporal lobe(s) hypoactivity
vii. Thalamic hyperactivity plus anterior cingulate hyperactivity

Directing treatment towards the functional abnormalities proved successful in achieving a response to treatment in many cases and remission in some cases. We present the clinical case and scan images of one such patient.
A 48 year old woman presented with a 12 year history of chronic Major Depressive Disorder that had not adequately responded to previous psychopharmacology and psychotherapy. Past medical history included hypothyroidism for several years, well treated and monitored. There was no history of substance abuse. Intake medications were venlafaxine-XR 300mg AM, bupropion-SR 150mg BID, and Eltroxin 0.1mg.
3D SPECT scan revealed bilateral perfusion defects in the infraorbital prefrontal cortex, a perfusion defect in the left antero-medial temporal lobe and hyperperfusion of the right basal ganglia and thalami.
Bupropion was increased to bupropion-XL 450mg AM for an increased dopaminergic effect directed towards the prefrontal cortex, and pregabalin 150mg HS was added directed towards the basal ganglia and thalami.
The patient improved clinically towards remission and has returned to work. Repeat 3D SPECT scan shows resolution of the prefrontal cortical defects and improvement of the left antero-medial temporal lobe defect.
Conclusions: Patients with a clinical diagnosis of Major Depressive Disorder can show varying patterns in their 3D SPECT scans. Targeting the psychopharmacology to the functional defects indicated by the SPECT scan can help patients with otherwise refractory Major Depressive Disorder to achieve a better response to treatment or even remission in some cases.

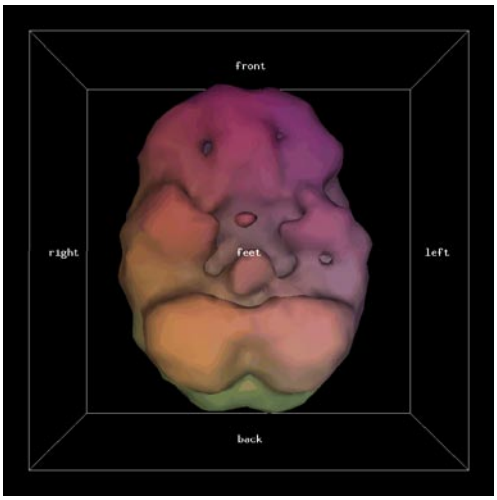

Initial 3D SPECT cortical view of inferior aspect of brain

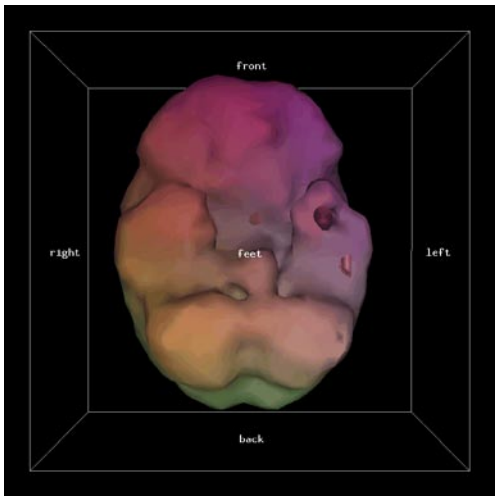

Post-treatment 3D SPECT cortical view of inferior aspect of brain

---

002

INTRAVENOUS ADMINISTRATION OF DIAZEPAM SIGNIFICANTLY REDUCES BROWN FAT ACTIVITY ON 18F-FDG PET/CT

Rajan Rakheja[1], Anthony Ciarallo[1], Yazan Z Alabed[1], Marc Hickeson[1]1) Department of Nuclear Medicine, Royal Victoria Hospital, Montreal, Quebec, Canada.

Brown adipose tissue (BAT) activity on 18F-fluorodeoxyglucose (FDG) PET/CT can introduce an undesirable element of complexity when attempting to discern physiologic activity from more ominous entities. Recent studies have demonstrated several methods to reduce BAT FDG uptake. Benzodiazepines, however, have yet to been proven effective against BAT.

Methods: Twenty-five patients with increased BAT FDG uptake were selected retrospectively from our PET/CT database between November 2004 and January 2011. These patients had been asked to return on a different day for repeat scanning with 5mg of intravenous diazepam, administered ten minutes prior to FDG. Two patients underwent this procedure on a second occasion (for a follow-up scan at a later date), thus resulting in a total of twenty-seven scans from twenty five patients. FDG uptake in BAT was recorded using the maximum standardized uptake value (SUVmax).

Results: The mean basal BAT SUVmax was 10.1 ± 4.6 compared to a mean SUVmax of 2.8 ± 3.3 post IV diazepam ($p < 0.0001$). Approximately 89% (24 of 27) of scans had no significant residual BAT activity. The three remaining scans had a reduction in SUVmax ranging from 23-64% following diazepam administration. No adverse effects were noted.

Conclusion: We observed a significant reduction in brown fat activity in para-spinal, cervical, mediastinal, para-adrenal, and supra- and infra-clavicular regions on PET/CT following premedication with intravenous diazepam.

We feel that IV benzodiazepines should be considered a pharmacologic option for reducing BAT FDG uptake, which in turn, will aid in distinguishing physiologic metabolic activity from pathology.

003

QUANTITATIVE PARAMETERS FOR A MODEL OF WHOLE BODY METABOLIC TUMOUR BURDEN IN PATIENTS WITH DIFFUSE LARGE B CELL LYMPHOMA USING PET/CT

Mathew Bligh, David MacDonald, Mohamed Abdolell, Steven Burrell

Objective: For patients with nodal diffuse large B cell lymphoma (DLBCL), we investigate correlation of PET/CT parameters SUVmax and SUVmean from staging scans with known prognostic indicators including cellular proliferation index Ki-67 and serum LDH, with the goal of developing a PET/CT-based scoring system for DLBCL prognosis. This PET/CT-based system would compliment or improve upon the International Prognostic Index (IPI) for non-Hodgkin lymphoma (NHL).
Methods: We searched our institution's PET database for patients with DLBCL having PET/CT scans for staging purposes. Of 57 patients identified, 40 were excluded due to coexisting cancers, prior treatment, lack of laboratory data or presence of extranodal disease. For the remaining 17 patients, PET/CT scans were evaluated for mean and maximum standardized uptake value (SUVmean, SUVmax) and volume for each tumour site. Medical records were searched for serum LDH and Ki-67. Ki-67 was compared with global SUVmax. As a preliminary exercise, we also proposed two scores accounting for both SUV and volume in each lesion, represented as a whole-body sum. These measures of total glycolysis (TG) were defined as: 1) TGmean = SUM(SUVmean×volume) and 2) TGmax = SUM(SUVmax×volume). These scores were compared to LDH and Ki-67, respectively. The Pearson correlation coefficient was used to assess correlation between continuous variables.
Results: A statistically significant positive correlation was demonstrated between Ki-67 and global SUVmax (ρ = 0.649, p=0.031), suggesting a relationship between biopsy-determined tumour aggressivity and global intensity of fluorodeoxyglucose (^{18}F-FDG) uptake. Neither LDH nor Ki-67 demonstrated correlation with our experimental TG scores.
Conclusions: This study represents an important first step in developing a PET-based prognostic model for DLBCL. Due to the limited study population, power was insufficient to reliably detect significant relationships. Our database will be expanded over the next 1-2 years, allowing us to investigate further and develop a prognostic model.

004

ROLE OF HIGH DEFINITION BRAIN SPECT IN THE EVALUATION OF NON-CONVULSIVE EPILEPSY VARIANTS WITH COMORBIDITY

Dan G Pavel, MD; Steven R. Best, MD; Y-C Chang MS.

Objective: The presence of comorbidity can delay appropriate treatment in non-convulsive epilepsy, even in the presence of nonspecific EEG findings which are often considered as not significant We have evaluated the impact of brain SPECT on patient management in such cases.

Methods Used: Triple head camera with fan beam collimators. Radiopharmaceutical: 99mTc-HMPAO. Multifaceted display including sections in 4 planes, multi-thresholded 3D views and normalized surface maps (Neurostat); discrete color code. 37 patients (age 12 – 59) with symptom duration of one to several years. None had previously had anti epileptic drugs (AED-s). EEG-s done with a reproducible protocol, interpreted by same expert.
Results: Among significant comorbidities, were one or more of : depression , anxiety, learning, memory, cognitive impairments, TBI or neurotoxic induced symptoms and sleep disorders. On SPECT displays the presence of hyper and / or hypoperfusion was evaluated in the hemispheres (global or focal), as well as in multiple subcortical structures . There were various combinations but the common denominator was the presence of one or multiple localized areas of marked and / or extreme hyperperfusion. This in turn influenced the choice of treatment which started with or added AED-s and, subsequently, continued with dose adjustments and additions of medications and/or of other methods. In 92 % of cases, the features detected on Brain SPECT provided a rationale for the clinical manifestations, contributed to the therapeutic strategy and also provided an explanation for past medication failures.
Conclusions: The presence and type of brain SPECT abnormalities has proven to be of clinical relevance in the evaluation and treatment of patients with non-convulsive epilepsy variants, with comorbidity.

005

COMPARISON OF EJECTION FRACTION USING MUGA SCANNING AND 3D ECHOCARDIOGRAPHY.
Peter A. Dutchak, Daniel Brouillard, Murray F. Matangi

Objective: To compare ejection fraction (EF) by 3D echocardiography (ECHO) and MUGA.
Methods: 68 patients referred for MUGA scanning also underwent 3D ECHO for measurement of EF. The 3D ECHO was performed first and was followed immediately by MUGA scanning. The 3D ECHO and MUGA scanning analysis for EF were performed by two separate investigators. 3D images were acquired using a GE VIVID E9 system with a 4V probe. These images were then analysed using the TOMTEC 4D LV volumes and EF analysis system. Each investigator was blinded to the EF results of the other. The EF data from 3D ECHO and MUGA scanning was then collected and analyzed. A paired t test was used to assess differences between the mean values for each method. A p value of <0.05 was considered statistically significant. A Bland-Altman scatter plot was used to assess the inter-changeability of the two methods. The methods were considered to be interchangeable if 95% of data points were within ± 1.95 standard deviations from the mean difference between the two methods.
Results: Of the 68 MUGA scans only 46 (68%) 3D ECHOs had analysable images. There were 13 females and 33 males with a mean age of 63.1 ± 15.1 years. The mean EF by MUGA was 47.2 ± 12.2% compared to 46.9 ± 10.6% for 3D echocardiography (P = 0.9001). The Bland-Altman scatter plot (see figure 1.) shows that 98% of data points lay within ± 1.95 standard deviations from the mean difference of the two methods.
Conclusion: When image quality allows, 3D ECHO offers a comparable alternative to MUGA scanning for the measurement of EF. The Bland-Altman scatter plot indicates these methods are interchangeable. This may have important clinical implications with respect to patients requiring frequent serial measurements of EF, which can be done, reliably in the absence of radiation exposure.

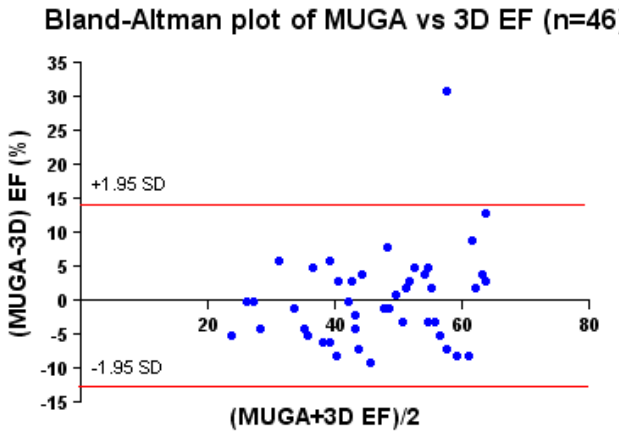

Figure 1.

006

FACTORS INFLUENCING NON-CARDIAC SIDE EFFECTS OF DIPYRIDAMOLE WHEN USED FOR MYOCARDIAL PERFUSION STRESS TESTING

Robert Miner BSc (MRS), M.R.T.(N.)[a] Ottawa Cardiovascular Centre, MSc candidate (MRS, nuclear medicine) Charles Sturt University*

Purpose: This study evaluates whether patient demographic information can be used to predict the side effects experienced during myocardial perfusion imaging (MPI) procedures using dipyridamole.

Method: Patients scheduled for myocardial perfusion pharmacological stress testing using dipyridamole were randomly selected. Patient demographic data: age, sex, BMI, diabetic status, smoker status and daily aspirin usage was collected before the start of the procedure.

Patients underwent a one day rest then pharmacological stress MPI procedure. ^{99m}Tc-Myoview or ^{201}Tl were used as the radiopharmaceutical. The pharmacological stress procedure used dipyridamole injections based on body weight. Aminophylline was injected at the end of the stress session. Once completed the procedure patients were given a questionnaire that asked them to report the severity of any side effects experienced from the dipyridamole. Data was analyzed using Chi-squared, Mann-Whitney, student t-test, multiple linear regression and multiple logistic regression tests.

Results: A total of 119 patients were surveyed (58 male, 61 female). The average age was 67.7 years (10.7 standard deviation). There were no statistically significant differences in the male and female demographics and physiological data except for daily aspirin usage (more common with males). In this investigation the frequency of specific side effects differed from some studies but agreed with others. Headaches were the most common side effect (50% of all patients), followed by dizziness (26%), flushing (24%), chest pain (19%) and nausea (18%). Correlations and associations were found between patients experiencing no side effects with age (r^2 = 0.369) and sex (p = 0.034); headaches with age (r^2 = 0.499) and BMI (r^2 = 0.215); chest pain with diabetic status (p = 0.017); dizziness with diabetic status (p = 0.039); and nausea with age (r^2 = 0.375).

Conclusion: Side effects of dipyridamole are generally known, but the factors influencing incidence and severity are not. This study has shown patient demographic information normally gathered before the MPI procedure can help predict the occurrence and severity of some side effects. Providing more accurate information on the possible side effects to a patient could help reduce patient anxiety and improve patient cooperation.

007

VALIDATION OF TIKHONOV ADAPTIVELY REGULARIZED GAMMA VARIATE FITTING WITH 24-HOUR PLASMA CLEARANCE IN CIRRHOTIC PATIENTS WITH ASCITES

Wesolowski, Carl A.[1]; Ling, Lin[1]; Xirouchakis, Elias[2]; Burniston, Maria T.[3]; Puetter, Richard C.[4]; Babyn, Paul S.[5]; Giamalis, Ioannis[2] and Burroughs, Andrew K.[2]1. Radiology, Memorial University of Newfoundland, St. John's, NL, Canada. 2. The Royal Free Sheila Sherlock Liver Centre, Royal Free Hospital, London, UK. 3. Department of Medical Physics, Royal Free Hampstead NHS Trust, London, England. 4. Center for Astrophysics & Space Sciences, University of California, San Diego, La Jolla, CA, United States. 5. Radiology, University of Saskatchewan, Saskatoon, SK, Canada.

Objectives: To compare late-time extrapolation of plasma clearance (*CL*) from Tikhonov adaptively regularized gamma variate fitting (Tk-GV) and from mono-exponential (E1) fitting.
Methods: Ten 51-Cr-EDTA bolus IV studies in adults–8 with ascites–assessed for liver transplantation, with 12 to 16 plasma samples drawn from 5-min to 24-hours were fit with Tk-GV and E1 models and *CL* results were compared using Passing-Bablok fitting.
Results: The 24-hr *CL*(Tk-GV) values ranged from 11.4 to 79.7 ml/min. Four-hour versus 24-hour *CL*(Tk-GV) plotting yielded no significant departure from a slope of 1, whereas the 4- versus 24-hr *CL*(E1) slope, 1.56, was significantly increased. The plot of *CL*(Tk-GV-24-hr) versus *CL*(E1-24-hr) had a biased slope and intercept (0.85, 5.97 ml/min). Moreover, the quality of fitting of 24-hr data was significantly better for Tk-GV than for E1, as follows. For 10 logarithm of concentration curves, higher *r* values were obtained for each Tk-GV fit (median 0.998) than for its corresponding E1 fit (median 0.965), with $P<0.0001$ (paired *t*-test of *z*-statistics from Fisher *r*-*z* transformations). The E1 fit quality degraded with increasing *V/W* (volume of distribution (l) per kg-body weight, $P=0.003$). However, Tk-GV fit quality versus *V/W* was uncorrelated ($P=0.8$).
Conclusions: *CL*(E1) values were dependent on sample time and the quality of fit degraded with increasing ascites. *CL*(Tk-GV) was relatively insensitive to sample time selection, had improved fit quality relative to E1, and was unaffected by ascites. Thus, the area under the curve (*AUC*) and *CL*(Tk-GV) values, calculated using *AUC*, were significantly more reliable than *CL*(E1) values.
Keywords: Renal function, Tikhonov regularization, Minimization of errors, Gamma variate, Ascites

Eric Lepp Clinical Vignettes

EL-001

HYPOMETABOLIC APPEARANCE OF CEREBRAL HISTOPLASMOSIS ON 18F-FDG PET/CT

Rajan Rakheja MD[1], Stephan Probst MD[1] 1), Division of Nuclear Medicine, Jewish General Hospital, Montreal, Quebec, Canada.

A 66-year-old HIV-positive woman presented with new onset headache, dizziness and unsteady gait. A MRI of the brain showed multiple ill-defined contrast-enhancing lesions for which the differential included high-grade astrocytoma, metastases but was felt less likely to represent infection. The patient then underwent 18F-FDG PET scanning to exclude a putative extra-axial primary neoplasm, however the PET study failed to show extra-cerebral FDG-avid lesions. The cerebral lesions described on MRI were hypometabolic as compared to normal gray matter, and thus we raised the likelihood of infection. Following the failure of a diagnostic-therapeutic trial of antimicrobials for toxoplasmosis, a brain biopsy confirmed histoplasmosis. Even in HIV patients, cerebral histoplasmosis with clinical symptoms is a rare entity and only a few case reports are present in the imaging literature[1,2]. Involvement of the CNS can occur in 5–20% of cases of disseminated histoplasmosis and presents as meningitis (40–60%), focal brain lesions (25%) and encephalitis (10%)[3]. CNS histoplasmosis can be very difficult to diagnose via conventional imaging modalities such as CT and MRI, as was the case with our patient. Often, the isolated brain lesion is thought to be a brain tumor or toxoplasmosis; these two entities represent approximately 80% of focal CNS lesions in AIDS patients[4]. Diagnosis is usually made by CSF culture or biopsy, however even these test have limitations; sensitivities range from 20–60% for CSF culture and 50–80% for tissue biopsy[5]. To the authors' knowledge, this represents the first 18F-FDG PET/CT study of histopathologically-proven cerebral histoplasmosis and serves to increase awareness of an infection in HIV/AIDS patients, which if misdiagnosed, could result in significant morbidity.

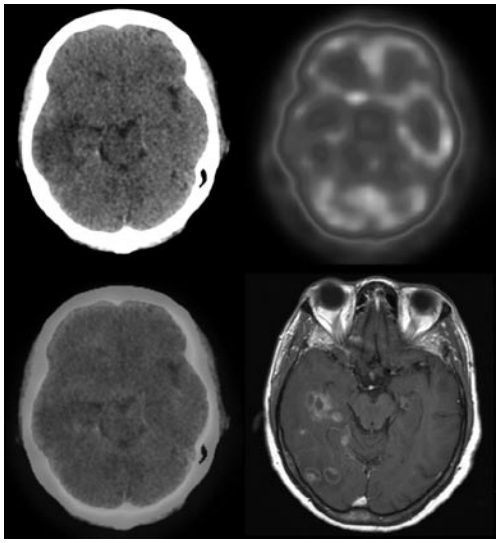

FIG 1: Figure one shows CT, PET, fused PET/CT, and MRI (T1 sequence post Gadolinium) transaxial images acquired 76 minutes following 12 mCi of 18F-FDG demonstrate hypometabolism in the right temporal lobe which correlated to the largest lesion described on MRI.

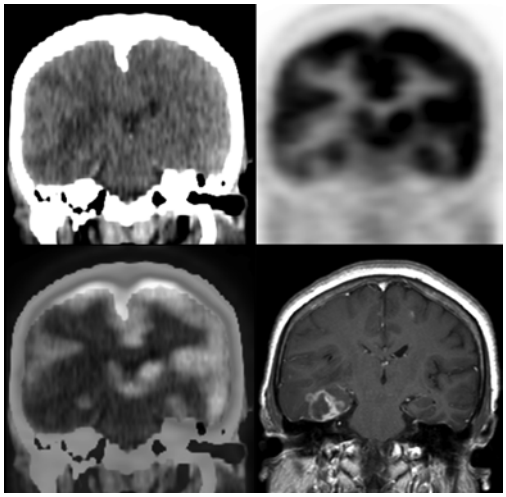

FIG 2: Figure two depicts CT, PET, fused PET/CT, and MRI (T1 sequence post Gadolinium) coronal images showing the largest lesion in the right temporal lobe measuring 2.4 x 1.9 cm which demonstrates irregular peripheral enhancement and correlates to the area of hypometabolism on PET.

References

1. Iraklis C and al. Clinical Evidence of Spinal and Cerebral Histoplasmosis Twenty Years after Renal Transplantation. Clinical Infectious Diseases Vol. 20, No. 3 (Mar., 1995), pp. 692-695
2. Klein, J. Mayo Clinic Proceedings August 1999 vol. 74 no. 8 803-807.
3. Wheat, LJ, Batteiger, BE, Sathapatayavongs, B. Histoplasma capsulatum infections of the central nervous system: A clinical review. Medicine (Baltimore) 1990; 69:244
4. Ciricillo, SF, Rosenblum, ML. Use of CT and MR imaging to distinguish intracranial lesions and to define the need for biopsy in AIDS patients. J Neurosurg 1990; 73:720.
5. Wheat, LJ, Current diagnosis of histoplasmosis, Trends Microbiol 11 (2003), pp. 488–494

EL-002

ROUND CELL LIPOSARCOMA PRESENTING AS AN FDG POSITIVE PRIMARY WITH A FDG NEGATIVE RETROPERITONEAL METASTASIS: A PITFALL FOR 18F-FDG PET/CT IMAGING

Rajan Rakheja MD[1], William Makis MD[2]

A 34-year-old man, who presented with a ten month history of a enlarging right ankle mass histologically proven to be a round cell/myxoid liposarcoma, was referred for an 18F-FDG PET/CT, which showed a heterogenous FDG-positive primary in the ankle, and a 1.2 cm FDG-negative retroperitoneal lipis-attenuating nodule. On a follow-up PET/CT done one year later, the retroperitoneal nodules had grown into a 11 cm mass, which became FDG-positive and was subsequently histologically confirmed to be a liposarcoma metastasis. We present the imaging characteristics of this highly unusual case, and a possible histological explanation for the false-negative retroperitoneal metastasis on the staging PET/CT.

Figure 1: A 34-year-old man presented with a ten month history of a enlarging right ankle mass which was revealed to be a round cell/myxoid liposarcoma on histopathological evaluation. (a) Maximum intensity projection (MIP) (b) coronal PET, (c) CT, and (d) PET/CT fusion images of an 18F-FDG PET showed intense but heterogeneous

FDG uptake in the 22 cm primary malignancy involving the soft tissues of the right lower leg and ankle. The most aggressive-appearing aspect of the sarcoma which exhibited necrosis and hemorrhage on gross pathology had a maximum standardized uptake value (SUV-max) of 5.3. However, the bulk of the mass showed milder FDG uptake with SUV-max of 2.5.

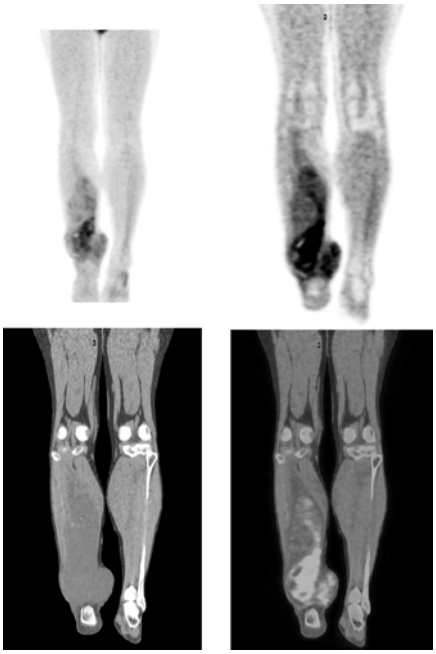

Figure 2: a) The gross pathology specimen showed a high grade round cell component (red arrows) arising from the lower grade myxoid liposarcoma (blue arrows). The area of intense FDG uptake in the region of the ankle, as seen in figure 1, corresponded well to the location of the high grade round cell component (multiple foci of tumour necrosis on a background of fleshy round cell myxoid liposarcoma is shown by the red arrows), while the remainder of the tumour that showed low or no FDG uptake corresponded to the low grade myxoid liposarcoma component (blue arrows).

Figure 3: The transaxial (a) CT, (b) PET, and (c) PET/CT fusion images of the staging PET/CT also showed a 1.2 cm right retroperitoneal nodule with no FDG uptake (arrow), which was felt to be an indeterminate finding. A follow-up PET/CT was performed one year after the staging PET/CT to assess response to therapy. (a) CT, (b) PET and (c)

PET/CT fusion images of the follow-up PET/CT showed a significant enlargement of the retroperitoneal nodule, now measuring 6 x 9 x 11 cm and showing FDG uptake with SUV-max of 2.3.
In our case, the round cell myxoid liposarcoma showed a range of mild and moderate 18F-FDG uptake with SUV-max from 2.5 to 5.3, excluding the small necrotic areas. It was therefore reasonable to expect that any metastases larger than the limit of spatial resolution for the PET/CT would also show FDG uptake within this SUV range. The 1.2 cm retroperitoneal nodule did not show any FDG uptake on the staging PET/CT, but developed into a 11 cm FDG positive metastasis on the follow-up study. To our knowledge, this is the first report of an FDG positive primary liposarcoma presenting concurrently with a falsely FDG negative retroperitoneal metastasis.

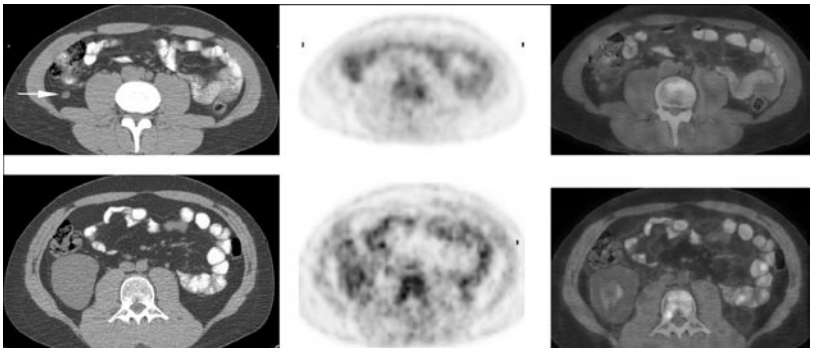

Figure 4: Both slides are A&B. Hematoxylin and Eosin stain; magnification x100
(a) Myxoid Liposarcoma of the lower leg. Shows that the bulk of the right lower leg primary liposarcoma has a hypocellular myxoid rich matrix with mild round cell proliferation and "chicken wire" capillaries characteristic of low grade myxoid liposarcoma. (b) Retroperitoneal metastasis biopsied after the follow-up PET/CT shows a much more hypercellular round cell proliferation devoid of myxoid matrix and lipoblasts consistent with round cell myxoid liposarcoma.
PET/CT readers should be aware that round cell myxoid liposarcomas can have FDG- positive or FDG- negative metastases, depending on the extent and cellularity of the high grade round cell component, regardless of how intense the FDG uptake is in the primary tumour. This is in contradistinction to other types of high grade sarcomas where the histology is uniformly high grade, correlating with a high SUV and higher sensitivity on PET/CT. This should be kept in mind as a potential pitfall in the evaluation of round cell/myxoid liposarcomas by 18F-FDG PET/CT and should encourage physicians to take into account the exact pathologic subtyping of sarcomas.